Crystal and magnetic structure of $TbNi_2Mn$

N. V. Mushnikov,[1,*] V. S. Gaviko,[1] J. Park,[2] and A. N. Pirogov[1,2,3]
[1]*Institute of Metal Physics, Ural Division, Russian Academy of Sciences, S. Kovalevskya 18, 620041 Ekaterinburg, Russia*
[2]*Department of Physics, SungKyunKwan University, 440-746 Suwon, Korea*
[3]*Center for Strongly Correlated Materials Research, Seoul National University, 151-742 Seoul, Korea*
(Received 16 January 2009; revised manuscript received 30 March 2009; published 19 May 2009)

The crystal and magnetic structures of the $TbNi_2Mn$ compound have been refined by the Rietveld analysis of neutron powder-diffraction data. The compound has a cubic C15b-type structure, in which Mn atoms partially occupy both the 4*a* and 16*e* sites. Bulk magnetization measurements revealed magnetic ordering below the Curie temperature $T_C=142$ K. The values of magnetic moment are different for the Tb ion at the 4*a* and 4*c* positions. In the 4*c* site, the Tb moment is determined to be $5.4\mu_B$/Tb ion. The low value of the Tb-ion moment is indicative of the formation of a random magnetic anisotropy.

DOI: 10.1103/PhysRevB.79.184419 PACS number(s): 75.25.+z, 61.05.fm, 61.05.cp

I. INTRODUCTION

Intermetallic compounds of rare-earth (*R*) and 3*d*-transition (*T*) metals with the Laves phase structure were the subject of extensive studies in the past decades owing to their relatively simple crystal structure and outstanding magnetic properties such as giant magnetostriction[1] and a large magnetocaloric effect.[2] The cubic $MgCu_2$-type Laves phase (C15, space group $Fd\bar{3}m$) is a close-packed structure, the formation of which is limited by the ratio of the atomic radii of the constituent elements (1.10 to 1.30) and the concentration of valence electrons per atom.[3,4] No homogeneity range is usually observed for the binary RT_2 compounds. However, the zirconium-based hexagonal C14-type compound $ZrMn_2$ has been reported to have a homogeneity region extending from $ZrMn_{1.8}$ to $ZrMn_{3.4}$.[5] The C15-type Laves phase was found in the $(Zr_{1-x}Mn_x)Co_{2+\delta}$ alloys for $0 \leq x < 0.2$.[6,7]

Recently, Wang *et al.*[8] found that the RNi_2Mn alloys with R=Tb, Dy, Ho, and Er crystallize in the $MgCu_2$-type structure. Their Curie temperatures (T_C) were found to be considerably higher than the T_C values of the corresponding RNi_2 and RMn_2 compounds. For RNi_2Mn compounds with different *R* atoms, T_C linearly depends on the de Gennes factor with the largest reported value $T_C=131$ K for $TbNi_2Mn$. This value is 3.5 and 2.4 times as large as that for $TbNi_2$ and $TbMn_2$ counterparts, respectively. The spontaneous magnetic moment of $TbNi_2Mn$ determined from the bulk magnetization measurements amounts to $4.8\mu_B$ per formula unit (f.u.),[8] which is considerably smaller than the value of $g_J J\mu_B = 9\mu_B$ for the free Tb^{3+} ion and $6.1-7.8\mu_B$/f.u. for $TbNi_2$ with the nonmagnetic Ni atoms.[9] Assuming that the Ni atoms give a negligible contribution to the magnetic moment of RNi_2Mn, Wang *et al.* suggested that the Mn atoms have a rather large magnetic moment directed opposite to the moment of the Tb atoms.

The magnetic behavior of nickel in *R*-Ni intermetallics has been a subject of debates. The formation of the *R*-Ni compound is accompanied by the 3*d*-5*d* hybridization and the charge transfer of the 5*d* electrons to the 3*d* band. As a result, the Ni magnetic moment collapses for most of the *R*-Ni compounds. However, accurate measurements show that magnetic heavy *R* atoms may induce a small magnetic moment of Ni. For the $(Gd_xY_{1-x})Ni_5$ series it was shown that nickel is not magnetically ordered in YNi_5, while an induced magnetic moment up to $0.16\mu_B$/Ni appears when Gd is substituted for Y.[10] Recently, the Ni magnetic moment oriented antiparallel to the rare-earth one was confirmed for $GdNi_2$ by using the magnetic Compton profile method.[11] For the RNi_2 compounds the exchange 4*f*-5*d*-3*d* interaction is rather weak and the Curie temperatures are rather low.[12] Observation of relatively high-T_C values for RNi_2Mn allows one to assume the appearance of the intrinsic magnetic moment on nickel atoms, which contradicts the accepted picture of magnetism of *R*-Ni compounds.

According to the Rietveld-refinement analysis of the x-ray diffraction patterns of $TbNi_2Mn$,[8] the Mn and Ni atoms seat in the 16*d* sites of the $MgCu_2$-type structure with the occupancies 25.9% and 74.1%, respectively. The 8*a* sites are not fully occupied by Tb atoms. About 22.2% of these sites are occupied by Mn atoms and 3.7% are empty. Since the Tb and Mn atoms have different atomic radii, such a structure can hardly be expected considering the generally recognized rules of formation of the Laves phase. A strong tendency to ordering was found for RNi_2 compounds with the *R* deficient compositions.[13,14] A cubic structure of RNi_2 with the regularly arranged vacancies on the *R* site is a superstructure (space group $F\bar{4}3m$) of the cubic Laves phase.[15] The ordering of the vacancies can be destroyed by application of external pressure or high temperature.[16] Because of a large difference in the metallic radii of *R* and Mn atoms, one can expect ordering of these atoms within the 8*a* sites in RNi_2Mn compounds.

In this paper, we present the results of x-ray and neutron-diffraction study of $TbNi_2Mn$. Our data suggest that the compound has the C15b ($AuBe_5$)-type structure. The 4*c* sites are fully occupied by Tb ions, while the remaining Tb and a part of Mn atoms randomly occupy the 4*a* sites. We determine the magnetic structure of the compounds and show that the Ni atoms possess a magnetic moment of at least $0.3\mu_B$. A reduced Tb-ion magnetic moment at 4.2 K as determined from the neutron diffraction and bulk magnetization measurements allows us to assume the formation of a local uniaxial magnetic anisotropy in the compound.

 ©2009 The American Physical Society

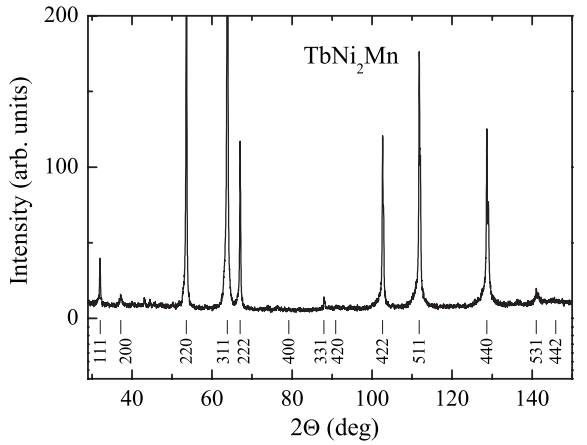

FIG. 1. X-ray diffraction pattern of the $TbNi_2Mn$ alloy.

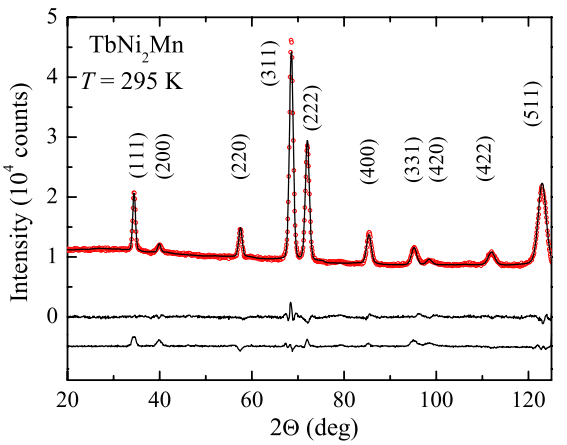

FIG. 2. (Color online) Room-temperature neutron-diffraction pattern of the $TbNi_2Mn$ alloy. Symbols represent experimental data. The line through these data points corresponds to the Rietveld analysis with the structural parameters listed in Table I. The line below shows the difference between the experimental and calculated intensities. The lowest line shows the difference for the model of crystal structure suggested in Ref. 8.

II. EXPERIMENT

The $TbNi_2Mn$ compound was prepared by induction melting of the pure elements in alumina crucible. An excess of Mn (5 wt %) was added to compensate the Mn evaporation during the melting and subsequent annealing. The as-cast samples were wrapped in Ta foils, sealed in an evacuated silica tube, and annealed at 870 °C for one week.

X-ray powder-diffraction measurements at room temperature have been performed on a DRON-type diffractometer with Cr $K\alpha$ radiation. Neutron powder-diffraction data were collected at temperatures 4.2 and 295 K on the D-3 diffractometer with the neutron wavelength $\lambda = 2.424$ Å at IMP, Zarechny. The data were refined using the program FULLPROF based on the Rietveld analysis.[17] Measurements of the magnetization curves were performed using an induction technique in pulsed magnetic fields up to 15 T with the pulse duration time of 8 ms in the temperature range 4.2–200 K. In order to take into account the demagnetizing field, we used the sample in the shape of a sphere of ~3 mm in diameter.

III. RESULTS AND DISCUSSION

A. Crystal structure

The room-temperature x-ray diffraction pattern presented in Fig. 1 confirms that the $TbNi_2Mn$ alloy crystallizes in the face-centered-cubic lattice. The lattice parameter $a = 7.184(1)$ Å almost coincides with that reported by Wang *et al.*[8] The most intensive lines can be indexed within the $Fd\bar{3}m$ space group of the C15 Laves phase. However, the diffraction pattern shows a few relatively weak reflections, such as (200) and (420), which are forbidden for the C15-type structure. These data imply that the structure of the $TbNi_2Mn$ alloy corresponds to a subgroup of the $Fd\bar{3}m$ space group. It should be noted that the x-ray diffraction pattern of $TbNi_2Mn$ presented in Ref. 8 also contained the (200) superstructure reflection at $2\Theta = 24°$ (Cu $K\alpha$ radiation), but it was attributed to an impurity phase.

Since the neutron-scattering lengths of Tb, Ni, and Mn atoms are substantially different (0.738, 1.03, and −0.373 [$\times 10^{-14}$ m]), the formation of the superstructure has to be evidenced more clearly in neutron-diffraction experiments. Figure 2 shows the neutron-diffraction pattern taken at room temperature which is much above the magnetic-ordering temperature. It can be seen that the superstructure (200) and (420) reflections have a much higher relative intensities than those for the x-ray diffraction pattern of Fig. 1. The best coincidence between the observed and calculated intensities of the neutron-diffraction pattern was achieved within the $F\bar{4}3m$ space group.

The C15b $AuBe_5$-type crystal structure with the $F\bar{4}3m$ space group is shown in Fig. 3. There are two kinds of Be sites (4*c* and 16*e*), and Au atoms occupy only the 4*a* sites. For the case when Tb and a part of the Mn atoms in $TbNi_2Mn$ are randomly distributed over the 4*a* and 4*c* sites, we obtain the disordered $MgCu_2$-type structure. The best refinement of the neutron-diffraction pattern has been obtained when we assume that the 4*c* sites are fully occupied by Tb atoms, while the 4*a* and 16*e* sites are occupied by Tb/Mn and Ni/Mn atoms, respectively. The agreement factors achieved are equal to $R_{Br} = 2.2\%$, $R_f = 1.6\%$, and $\chi^2 = 3.3$. The best refinement results are shown in Fig. 2. The atomic positions and site-occupancy factors are listed in Table I. Ac-

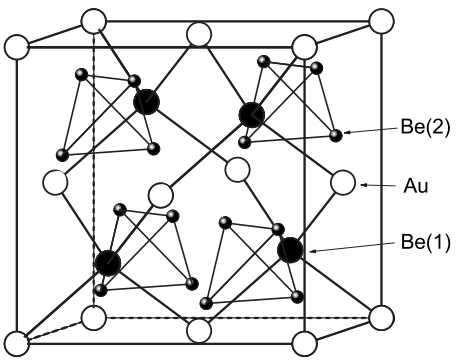

FIG. 3. Crystal structure of $AuBe_5$ (C15b) type.

TABLE I. Results of the refinement of room-temperature neutron-diffraction pattern for the atomic positions and site occupancies in the C15b unit cell of the $TbNi_2Mn$ compound (a =7.1842 Å, R_{Br}=2.2%, R_f=1.6%, χ^2=3.3).

Atom	Position	x/a	y/a	z/a	Occupancy coefficient at 295 K
Tb	4*a*	0	0	0	0.538(1)
Mn	4*a*	0	0	0	0.462(1)
Tb	4*c*	0.25	0.25	0.25	1.0
Mn	16*e*	0.624(1)	0.624(1)	0.624(1)	0.196(1)
Ni	16*e*	0.624(1)	0.624(1)	0.624(1)	0.804(1)

cording to these data, the chemical formula of the compound can be rewritten as $(Tb_4)^{4c}(Tb_{2.15}Mn_{1.85})^{4a}(Ni_{12.86}Mn_{3.14})^{16e}$ which corresponds to the composition $TbNi_{2.09}Mn_{0.81}$. Our attempts to fix the composition $TbNi_2Mn$ and/or to introduce vacancies lead to an increase in the agreement factors.

In order to clarify the difference between our model of the crystal structure of $TbNi_2Mn$ and that suggested in Ref. 8, we performed the Rietveld-refinement analysis of our neutron-diffraction patterns within the $MgCu_2$-type structure with the site-occupancy factors listed in Ref. 8. The deterioration of the goodness-of-fit procedure, which is evidenced by the lowest curve in Fig. 2, and the increase, for example, in the R_{Br} factor up to 7.66% implies that the model of the $AuBe_5$-type structure with $F\bar{4}3m$ space group is more adequate for the $TbNi_2Mn$ compound.

B. Magnetic structure and properties

Figure 4 shows magnetization curves of the $TbNi_2Mn$ sample measured at different temperatures. The sample shows no anomalies that can be associated with the field-induced magnetic transitions. The Curie temperature determined from the Arrot plots amounts to 142 K. This is an intermediate value between those previously reported for $TbNi_2Mn$, 131 K (Ref. 8), and 151 K.[18] The reasons for this difference are likely due to the difference in sample preparation technique, as well as in the compositions of these nonstoichiometric alloys.

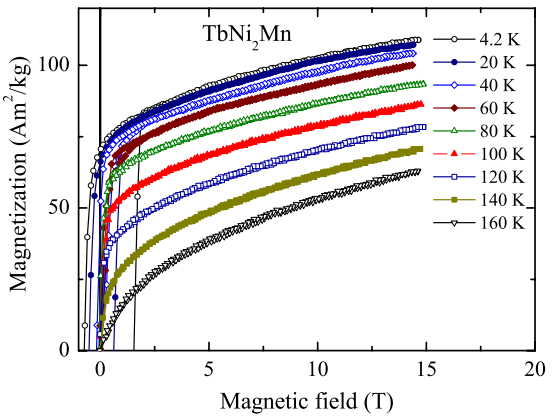

FIG. 4. (Color online) Magnetization curves of $TbNi_2Mn$ at different temperatures.

Using the Arrot plot we determine the spontaneous magnetization M_s=79 Am^2/kg at 4.2 K. This value corresponds to the spontaneous magnetic moment μ_s=4.7μ_B/f.u. A close value of 4.8μ_B/f.u. for $TbNi_2Mn$ was reported by Wang *et al.*,[8] while a larger saturation moment 5.59μ_B/f.u. was determined in Ref. 18.

The magnetization curves show no tendency to saturation in magnetic fields up to 15 T (Fig. 4). This may be due to several reasons. First, it may be caused by a polycrystalline structure of the studied sample. For a random cubic sample with a high magnetic anisotropy, the ratio of the spontaneous to saturation magnetizations is 0.831 for the easy [100] axis and 0.866 for the easy [111] axis. However, for $TbNi_2Mn$ at 4.2 K, the relation of M_s to the magnetization in the field 15 T($M_{15\ T}$) gives the value $M_s/M_{15\ T}$=0.72. Second, the high-field susceptibility may be due to a canting of the Tb and T sublattices of the ferrimagnet, if the Tb-Mn (Ni) exchange interaction is weak. This interaction can be estimated from the dependence of the T_C of the RNi_2Mn compounds with different R ions on the de Gennes factor $G=(g-1)^2J(J+1)$.[8] Extrapolation of this dependence to G=0 yields the contribution of the T-T exchange interaction to the Curie temperature as, approximately, 30 K. Considering the Curie temperature of $TbNi_2Mn$ to be 142 K, we can assume that the contribution of ~110 K is associated with the Tb-Mn (Ni) exchange interaction. The exchange field of this interaction can be estimated as 165 T. Since the average moment of the 3*d* sublattice is 1.7μ_B/f.u. (see below), the increase in the magnetization due to the sublattice canting should not exceed 3.4μ_B/f.u. in the field 165 T. For the applied field of 15 T we can expect the maximum magnetization growth from 79 to 84 Am^2/kg which is much smaller than that observed experimentally. Finally, if we assume that the zero-field magnetic structure is noncollinear, the high-field magnetic susceptibility may be due to a gradual alignment of the noncollinear magnetic moments.

The magnetic structure of $TbNi_2Mn$ has been determined from the powder neutron-diffraction pattern at 4.2 K presented in Fig. 5. As it follows from the comparison of Figs. 2 and 5, both the low- and high-temperature neutron diagrams contain the same reflections. Therefore, the wave vector of a magnetic structure is $\mathbf{k}$=0. Using this $\mathbf{k}$ value, we performed a symmetric analysis of magnetic structures which could be realized in the $TbNi_2Mn$ compound. The results of the analysis are presented in Tables II and III.

It was found that the ordering of magnetic moments at both 4*a* and 4*c* sites is described by the basis functions of the only irreducible representation τ_5 (Table II). Within this representation, the magnetic moments can be oriented along the edges ⟨100⟩, face diagonals ⟨110⟩, and space diagonals ⟨111⟩ of the crystal unit cell. Only a collinear alignment of the moments is allowed.

For the 16*e* sites, a wide variety of the magnetic structures can appear. As one can see from Table III, the magnetic ordering of the moments at the 16*e* position may be both ferromagnetic (τ_5) and antiferromagnetic (τ_2, τ_3, τ_4, and τ_5'). We performed the refinement of the experimental neutron-diffraction pattern of Fig. 5 for different combinations of the

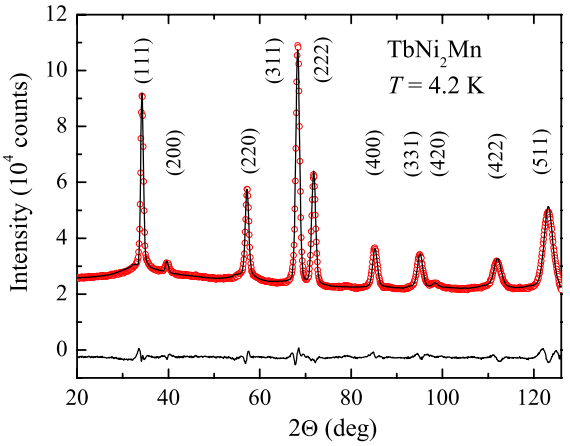

FIG. 5. (Color online) Neutron-diffraction pattern of $TbNi_2Mn$ at 4.2 K. Symbols represent experimental data. The line through these data points corresponds to the Rietveld refinement. The lowest line shows the difference between the experimental and calculated intensities.

basis functions. The minimum values of the agreement factors (χ^2=12.8, R_{Br}=3.5%, R_f=2.5%, and R_{mag}=5.3%) are achieved for the magnetic structure described by the basis functions of the τ_5 representation for all the crystallographic sites. For this structure, the average magnetic moments of the ions occupying the 4*a* and 4*c* sites are parallel to each other, but they are antiparallel to the moments at the 16*e* positions. The refined values of the average moments at the 4*a*, 4*c*, and 16*e* positions are equal to μ_a=4.2(2), μ_c=5.4(2), and μ_e =0.49(3)μ_B, respectively. The total magnetic moment is 5.0(7)μ_B/f.u., which is in satisfactory agreement with the results of the bulk magnetization measurements (4.7μ_B/f.u.).

Since we used powder unpolarized neutron diffraction, we cannot distinguish how the magnetic moments are oriented relative to the crystallographic axes. X-ray diffraction study of the aligned sample, which is a standard way of determining of the easy magnetization direction, cannot be applied to the paramagnetic at room-temperature $TbNi_2Mn$ compound with the cubic lattice. It should be noted that the Laves phase TbT_2 compounds for T=Ni, Co, Fe have the ⟨111⟩-type easy axis.[9,19,20]

In order to determine the values of the Tb-, Mn-, and Ni-ion moments from the average moments at the 4*a*, 4*c*, and 16*e* sites we have to make several additional assumptions. To reduce the number of variables we postulate the moments of Mn atoms at the 4*a* and 16*e* positions to be the same. The Ni ions are known to possess only a small induced moment in the RNi_2 compounds.[11] However, if we assume μ_{Ni}=0 for $TbNi_2Mn$ then the Tb moment at the 4*a* position exceeds its free-ion value 9μ_B for all the considered models of the magnetic structure. To reduce the Tb moment we have to accept that Ni ions possess magnetic moment in $TbNi_2Mn$. This result can be explained qualitatively by a change in a number of 3*d* electrons. Since Mn has less 3*d* electrons than Ni, alloying with Mn may cause electron transfer from the Ni to the Mn 3*d* subband, which may lead to splitting the Ni subband. On the other hand, the appearance of the Ni magnetic moment will lead to an increase in both *T*-*T* and *R*-*T* exchange interactions, which corroborate well with the observed growth of the Curie temperature.

Using the above assumptions and the occupation coefficients listed in Table I, we obtained the values of the Tb-ion moments at the 4*a* and 4*c* sites to be 9.0 and 5.4(2)μ_B, respectively. The Mn- and Ni-ion magnetic moments are equal to 1.4(2) and 0.3(2)μ_B, respectively. Here, the Ni moment is the minimum required for the Tb moment to not exceed its free-ion value.

A reduced average Tb-ion magnetic moment of 5.4μ_B for the 4*c* site implies that some of the Tb moments deviate from the average magnetization direction. Owing to a random occupation of a part of the 4*a* sites by the Mn ions, the local easy axes for the Tb atoms at the 4*c* sites may be randomly distributed over the crystal. The complete field-induced alignment will lead to the increase in the Tb-ion moment at 4*c* position up to 9μ_B/atom, which causes the magnetization growth from 79 up to 123 Am^2/kg. This estimation is in agreement with the observed behavior of the high-field magnetization curves of $TbNi_2Mn$ at low temperature (Fig. 4).

The partial magnetic disordering in $TbNi_2Mn$ is evidenced also by a presence of broad maxima of the diffusive scattering on the neutron diagram recorded at 4.2 K (see Fig. 5). These maxima can be clearly seen near the Bragg (111) and (220) reflections. Since the intensity of these reflections depend, mainly, on the Tb-ion magnetic moments, one can assume that the diffusive maxima near the (111) and (220) reflections originate from fluctuations of the Tb-ion magnetic moments. The correlated length of the fluctuations, estimated from the half width of the diffusive maximum near the (111) reflection, is equal to approximately 7–10 Å. The long-range magnetic order in $TbNi_2Mn$ is affected by the short-range magnetic fluctuations which are localized within the elementary cell.

TABLE II. Basis functions of the irreducible representations of the space group $F\bar{4}3m$ at the positions 4*a* and 4*c* for the wave vector **k**=0.

	Atom			
Representation	1(0, 0, 0) 1(0.25, 0.25, 0.25)	2(0, 0.5, 0.5) 2(0.25, 0.75, 0.75)	3(0.5, 0, 0.5) 3(0.75, 0.25, 0.75)	4(0.5, 0.5, 0) 4(0.75, 0.75, 0.25)
τ_5	$(r,0,0)^a$ $(0,r,0)$ $(0,0,r)$	$(r,0,0)$ $(0,r,0)$ $(0,0,r)$	$(r,0,0)$ $(0,r,0)$ $(0,0,r)$	$(r,0,0)$ $(0,r,0)$ $(0,0,r)$

[a] r=0.333.

TABLE III. Basis functions of the irreducible representations of the space group $F\bar{4}3m$ at the position 16*e* for the wave vector $\mathbf{k}=0$.

	Atom			
	1(0.62, 0.62, 0.62)	2(0.62, 0.37, 0.37)	3(0.37, 0.62, 0.37)	4(0.37, 0.37, 0.62)
	5(0.62, 0.12, 0.12)	6(0.62, 0.87, 0.87)	7(0.37, 0.12, 0.87)	8(0.37, 0.87, 0.12)
	9(0.12, 0.62, 0.12)	10(0.12, 0.37, 0.87)	11(0.87, 0.62, 0.87)	12(0.87, 0.37, 0.12)
Representation	13(0.12, 0.12, 0.62)	14(0.12, 0.87, 0.37)	15(0.87, 0.12, 0.37)	16(0.87, 0.87, 0.62)
τ_2	(r,r,r) [a]	$(r,-r,-r)$	$(-r,r,-r)$	$(-r,-r,r)$
τ_3	$(u,-v+wi,-v-wi)$ [b]	$(u,v-wi,v+wi)$	$(-u,-v+wi,v+wi)$	$(-u,v-wi,-v-wi)$
	$(v-wi,-u,v+wi)$	$(v-wi,u,-v-wi)$	$(-v+wi,-u,-v-wi)$	$(-v+wi,u,v+wi)$
τ_4	$(0,u,-u)$	$(0,-u,u)$	$(0,-u,-u)$	$(0,u,u)$
	$(-u,0,u)$	$(u,0,u)$	$(u,0,-u)$	$(-u,0,-u)$
	$(u,-u,0)$	$(-u,-u,0)$	$(u,u,0)$	$(-u,u,0)$
τ_5	$(r,0,0)$	$(r,0,0)$	$(r,0,0)$	$(r,0,0)$
	$(0,r,0)$	$(0,r,0)$	$(0,r,0)$	$(0,r,0)$
	$(0,0,r)$	$(0,0,r)$	$(0,0,r)$	$(0,0,r)$
τ_5'	$(0,u,u)$	$(0,-u,-u)$	$(0,-u,u)$	$(0,u,-u)$
	$(u,0,u)$	$(-u,0,u)$	$(-u,0,-u)$	$(u,0,-u)$
	$(u,u,0)$	$(-u,u,0)$	$(u,-u,0)$	$(-u,-u,0)$

[a] $r=0.333$.

[b] $u=0.167$, $v=0.083$, and $w=0.144$.

IV. CONCLUSION

In summary, we studied a $TbNi_2Mn$ compound by x-ray, neutron diffraction, and bulk magnetization measurements. We found the superstructure reflections in both x-ray and neutron-diffraction patterns, which indicate that the compound has the $AuBe_5$-type structure (space group $F\bar{4}3m$) rather than the $MgCu_2$-type Laves phase structure suggested previously. The magnetic structure can be described by the basis functions of the τ_5 irreducible representation as an antiparallel ferrimagnetic ordering of the averaged Tb, Mn, and Ni moments. The Ni atoms possess a magnetic moment of at least $0.3\mu_B$. It is the appearance of the Ni magnetic moment that may be responsible for the observed drastic increase in the Curie temperature of $TbNi_2Mn$ in comparison with that of $TbNi_2$. However, the magnetic structure of $TbNi_2Mn$ cannot be considered as a simple collinear ferrimagnet. The Tb magnetic moment in the 4*c* site is considerably reduced. The neutron-diffraction patterns at 4.2 K indicate strong magnetic fluctuations with the correlation length of 7–10 Å. The magnetization curves exhibit an enhanced high-field susceptibility and no saturation in magnetic fields up to 15 T. All these features are attributed to the formation of a random magnetic anisotropy and noncollinear arrangement of the Tb-ion magnetic moments at the 4*c* position.

ACKNOWLEDGMENTS

This work was done within RAS Program (Projects No. 01.2.006 13391 and No. 01.2.006 13394), with partial support of Russian Foundation for Basic Research (Project No. 07-02-00219), Program of Neutron Investigation of Matter, Program of Presidium of RAS No. 5, and Swiss SCOPES Project No. IB7420-110849. Work at Sungkyunkwan University were supported by the BAERI program and 21st Century Frontier R&D Program for Hydrogen Energy.

*mushnikov@imp.uran.ru

[1] G. Engdahl, *Handbook of Giant Magnetostrictive Materials* (Academic, New York, 2000).

[2] K. A. Gschneidner, Jr., V. K. Pecharsky, and A. O. Tsokol, Rep. Prog. Phys. **68**, 1479 (2005).

[3] K. N. R. Taylor, Adv. Phys. **20**, 551 (1971).

[4] F. Stein, M. Palm, and G. Sauthoff, Intermetallics **12**, 713 (2004); **13**, 1056 (2005).

[5] R. M. van Essen and K. H. J. Buschow, Mater. Res. Bull. **15**, 1149 (1980).

[6] A. M. Gabay and V. S. Gaviko, J. Magn. Magn. Mater. **260**, 425 (2003).
[7] E. Sherstobitova, A. Vokhmyanin, A. Gabay, and J.-G. Park, Physica B **350**, E147 (2004).
[8] J. L. Wang, C. Marquina, M. R. Ibarra, and G. H. Wu, Phys. Rev. B **73**, 094436 (2006).
[9] E. Gratz, E. Goremychkin, M. Latroche, G. Hilscher, M. Rotter, H. Muller, A. Lindbaum, H. Michor, V. Paul-Bonocour, and T. Fernandez-Dias, J. Phys.: Condens. Matter **11**, 7893 (1999).
[10] D. Gignoux, D. Givord, and A. Del Moral, Solid State Commun. **19**, 891 (1976).
[11] K. Yano, Y. Tanaka, I. Matsumoto, I. Umehara, K. Sato, H. Adachi, and H. Kawata, J. Phys.: Condens. Matter **18**, 6891 (2006).
[12] E. Burzo and L. Chioncel, J. Optoelectron. Adv. Mater. **6**, 917 (2004).
[13] V. Paul-Boncour, A. Lindbaum, M. Latroche, and S. Heathman, Intermetallics **14**, 483 (2006).
[14] A. Lindbaum, J. Hafner, and E. Gratz, J. Phys.: Condens. Matter **11**, 1177 (1999).
[15] E. Gratz, A. Kottar, A. Lindbaum, M. Mantler, M. Latroche, V. Paul-Boncour, M. Acet, Cl. Barner, W. B. Holzapfel, V. Pacheco, and K. Yvon, J. Phys.: Condens. Matter **8**, 8351 (1996).
[16] A. Lindbaum, E. Gratz, and S. Heathman, Phys. Rev. B **65**, 134114 (2002).
[17] J. Rodriguez-Carvajal, Physica B **192**, 55 (1993).
[18] D. D. Jackson, S. K. McCall, S. T. Weir, A. B. Karki, D. P. Young, W. Qiu, and Y. K. Vohra, Phys. Rev. B **75**, 224422 (2007).
[19] D. Gignoux, F. Givord, R. Perrier de la Bathie, and F. Sayetat, J. Phys. F: Met. Phys. **9**, 763 (1979).
[20] A. E. Clark, in *Handbook on the Physics and Chemistry of Rare Earths*, edited by K. A. Gschneidner, Jr. and L. Eyring (North-Holland, Amsterdam, 1979), Vol. 2, p. 231.